



Behavior of ammonium adsorption by clay mineral halloysite

Qing-xiu JING^{1,2}, Li-yuan CHAI¹, Xiao-dong HUANG², Chong-jian TANG¹, Huan GUO², Wei WANG²

1. School of Metallurgy and Environment, Central South University, Changsha 410083, China;

2. School of Metallurgical and Chemical Engineering,
Jiangxi University of Science and Technology, Ganzhou 341000, China

Received 30 May 2016; accepted 10 January 2017

Abstract: Ammonium pollution becomes severe during mining of ionic rare earth-ores in southern China. As one of the main clay minerals in soils of ionic rare earth mines, halloysite plays an important role in ammonium adsorption. In this study, the saturated adsorption capacity, factors affecting adsorption and adsorption kinetics of halloysite for ammonium were investigated. The results indicated that the ammonium adsorption of halloysite was saturated with 1.66 mg/g at 303 K, pH of 5.6 and initial ammonium concentration of 600 mg/L (about half of the actual initial in-situ leaching concentration). When the initial concentration of $\text{NH}_4^+\text{-N}$, pH values and temperatures (288 K to 313 K) increased, the ammonium adsorption capacity of halloysite increased. The ammonium isothermal adsorption of halloysite matched the Langmuir and Freundlich isotherms. The adsorption process of ionic rare earth mining soils for ammonium was favorable. And the adsorption process followed closely the pseudo-second kinetic equation.

Key words: ionic rare earth mining area; halloysite; ammonium pollution; adsorption; dynamics

1 Introduction

Ionic rare earth ore is a unique and strategic resource of southern China. Under geological processes in warm and humid climate, granodioritic and volcanic rocks are weathered and transformed into clay minerals such as kaolinite, halloysite and illite. Rare earth elements are also released from the original rocks during the same geological events, forming REE-hydroxyl aqueous ions adsorbed on clay minerals. This process leads to the formation of ionic rare earth ore [1–3].

Current rare earth mining practices in southern China mainly involve in-situ leaching of ionic rare earth ores and ionic exchange by ammonium sulfate [4,5]. Ammonium adsorption by the soils within the mining area occurs with seeping and leakage of the leaching agent. Therefore, NH_4^+ is constantly accumulating and remains in the soil after the cessation of mining, leading to contents higher than 2000 mg/kg. This process inflicts great damage to the mine ecosystem. More severe $\text{NH}_4^+\text{-N}$ pollution happens under the action of rainfall

which induces serious eutrophication and other issues [6–8]. In the rare earth mining province of Jiangxi, China, a partial water quality monitoring of a section of the Zhangjiang and Gongjiang rivers revealed that NH_4^+ concentrations exceeded the national standard [9,10]. In specific key areas of ionic rare earth mining in the Three South Regions of Gannan (Longnan, Dingnan and Quannan), the ammonium pollution was severer. The water quality reached grade IV, exceeding substantially the national II grade. This is a problem closely related to the long-term exploitation of local ionic rare earth deposits. In China, tens of millions of tons of ionic rare earth raw ore are leached and exploited each year. The ammonium pollution from the mining areas, surrounding soils and then from surface and underground water will become severer. Moreover, effective techniques to prevent ammonium soil pollution are still lacking. In fact, $\text{NH}_4^+\text{-N}$ exists in two forms within the mined soil. The first one is associated with leaking solution of ammonium sulfate, and the other form relates to the adsorption onto clay minerals. Adsorption being a complex process [11,12], it is very important to study

Foundation item: Project (51674305) supported by the National Natural Science Foundation of China; Project (1602FKDC007) supported by Science and Technology Program of Gansu Province, China; Project (NSFJ2015-K06) supported by the Jiangxi University of Science and Technology, China

Corresponding author: Chong-jian TANG; Tel: +86-731-88830511; E-mail: chtang@csu.edu.cn

DOI: 10.1016/S1003-6326(17)60185-7

and decipher the ammonium adsorption characteristics of the soil clay minerals associated with ionic rare earth mining.

Halloysite is one of the principal clay minerals present in rare earth-bearing soils. Halloysite is a silicate mineral with a principal chemical formula given by $\text{Al}_2\text{Si}_2\text{O}_5(\text{OH})_4 \cdot n\text{H}_2\text{O}$. It is a natural nanotube material (halloysite nanotubes) [13]. It is the unique nanotube structure of halloysite that provides a strong adsorption capability for ammonium and other cations, due to its high porosity, large pore volume, light weight, low bulk density, high specific area, strong adsorption, high activity, etc. [13]. Therefore, the researches about the adsorption properties of halloysite have been reported by some domestic and foreign researchers.

KIANI [14] investigated the characteristics of silver ions adsorption in aqueous solution by halloysite nanotubes. The results showed that the nanotubes could be used as effective nano-adsorbents to remove heavy metal ions. LI et al [15] studied the removal of radiocobalt from waste waters by a natural halloysite clay mineral. They revealed that the halloysite had a good potential for cost-effective disposal of cobalt-bearing waste water. VISERAS et al [16] studied the adsorption characteristics of halloysite for 5-amino salicylic acids. They found that the overall adsorption process of 5-ASA by halloysite was attributed to two separate processes. KIANI et al [17] reviewed the influencing factors and kinetics characteristics of the adsorption of a malachite green cationic dye by halloysite.

However, the mechanisms of ammonium adsorption and adsorption involving halloysite present in rare earth-bearing soils are still not very clear. Therefore, an in-situ local halloysite clay mineral related to the residual weathered product of granite was selected as an ammonium adsorbent in this work. The saturated adsorption capacity, factors affecting the adsorption, isothermal adsorption and adsorption kinetics were studied taking into account the properties of the actual mined soil and the process practice of leaching. The research is expected to provide a theoretical basis for the action of $\text{NH}_4^+ - \text{N}$ in a mined soil, and to contribute a theoretical basis to develop technologies preventing ammonium pollution during mining for ionic rare earth-rich soils.

2 Experimental

2.1 Materials

The halloysite clay material used in the experiments was provided by a geological survey company mined from soils near to local ionic rare earth mines. The chemical composition (mass fraction, %) of halloysite is:

SiO_2 43.49, Al_2O_3 35.80, Fe_2O_3 1.20, MgO 0.52, SO_2 1.17, K_2O 0.24, Na_2O 0.02, H_2O 2.55. After being fine ground, the halloysite material was sieved and dried. A NH_4Cl guaranteed experimental reagent was used, whereas the other reagents were of analytical grade unless otherwise stated.

2.2 Adsorption methods

Static adsorption: two types of ammonium solutions having different initial $\text{NH}_4^+ - \text{N}$ concentrations or different pH values were prepared using an ammonium chloride reagent. 50 mL of each solution was measured and transferred into a 100 mL polyethylene bottle with a stopper. Halloysite adsorbent (1.0 g) was then added to each bottle. After being mixed uniformly, the suspension was agitated at 303 K for 5 h. Afterwards, the material in suspension was extracted and centrifuged at 9000 r/min for 20 min to get separation and the product passed through a 0.45 μm filter membrane. Finally, the supernatant was analyzed to obtain the $\text{NH}_4^+ - \text{N}$ concentration (C_e) using the Nessler reagent spectrophotometric procedure. The amount of the ammonium adsorbed per unit mass of the adsorbent, Q_e , at equilibrium can be calculated through Eq. (1). During the segment of this experiment, the effects of the initial ammonium concentrations and pH values on the adsorption capacity, Q_e , were investigated keeping the other parameters invariable.

$$Q_e = (C_0 - C_e)V/m \quad (1)$$

where Q_e is the amount of adsorbed ammonium per unit mass of the adsorbent (mg/g) at equilibrium; C_0 is the initial concentration of ammonium in solution before adsorption (mg/L); C_e is the concentration of ammonium in the solution at equilibrium (mg/L); V is the volume of the adsorption solution (mL); and m is the mass of the adsorbent (g).

Dynamic adsorption: some amount of ammonium solution with a given initial $\text{NH}_4^+ - \text{N}$ concentration was prepared with an ammonium chloride reagent. 50 mL of the solution was measured and transferred into a 100 mL polyethylene bottle. The operation was repeated several times. After the solutions were adjusted to a given pH value, 1.0 g of halloysite adsorbent was then added to each polyethylene bottle. After being mixed uniformly, the suspension was agitated at a set temperature. Afterwards, the suspensions were extracted at different time intervals. The suspensions were centrifuged, separated and filtrated, and the supernatants were analyzed for the concentration of ammonium (C_t). The Q_t value which represents the amount of ammonium adsorption after a contact time (t) was calculated through Eq. (2). During this analytical segment, we evaluated the effect of contact time and initial ammonium concentration. Furthermore, the effect of contact time

and temperature on adsorption was also evaluated, keeping other parameters invariable.

$$Q_t = (C_0 - C_t)V/m \quad (2)$$

where C_t is the ammonium concentration in solution (mg/L) after a contact time (t); Q_t is the amount of ammonium adsorbed per unit mass of the adsorbent (mg/g) after a contact time t .

2.3 Isothermal adsorption methods

Ammonium solutions with different initial concentrations of 10, 20, 50, 100, 200 and 300 mg/L were prepared and 50 mL of each solution was mixed with 1.0 g of halloysite adsorbent. Afterwards, the suspension was adjusted to a similar pH value and agitated at a set temperature for 5 h. After the suspension was centrifuged, separated and filtrated, the ammonium concentration in the supernatant was determined (C_e), and the Q_e value was calculated through Eq. (1).

The aforementioned experiments were carried out at 288, 293, 303 and 313 K, respectively.

2.4 Kinetic adsorption methods

Some amount of a $\text{NH}_4^+ - \text{N}$ solution having an initial concentration of 100 mg/L and a pH value of 5.6 was prepared. 50 mL of the solution was transferred into a 100 mL polyethylene bottle and mixed with 1.0 g of halloysite adsorbent. After several mixtures were prepared, they were agitated at a set temperature, and extracted at different time intervals of $t=10, 20, 30, 60, 120$ min, respectively. After being centrifuged separated and filtrated, the supernatant was analyzed, the ammonium concentration (C_t) and the Q_t value were calculated using Eq. (2). The aforementioned experiments were carried out at 288, 293, 303 and 313 K, respectively.

We have chosen pseudo-first-order, pseudo-second-order and intra-particle diffusion models to evaluate the kinetics characteristics of ammonium adsorption by halloysite following the experimental data.

2.5 Analytical methods

The morphology and structure of halloysite samples were determined by scanning electron microscopy (SEM, MLA650F, USA FEI). Their crystal structure was established by X-ray diffractometry (XRD, Empyrean, PANalytical company with a Cu target, using the K_α radiation, a wavelength λ of 0.1542 nm and range in angle from 5° to 80°). The samples group structure was analyzed by Fourier transform infrared spectroscopy (FT-IR, ALPHA, Bruker Corporation) with a sample: KBr mass ratio of 1:100. The ammonium concentration in solution was measured by UV visible spectrophotometry (UV-2802, UNICO (Shanghai) Instrument Co., Ltd.).

3 Results and discussion

3.1 Characteristics of halloysite

The results of SEM, XRD and FT-IR are presented in Figs. 1, 2 and 3, respectively.

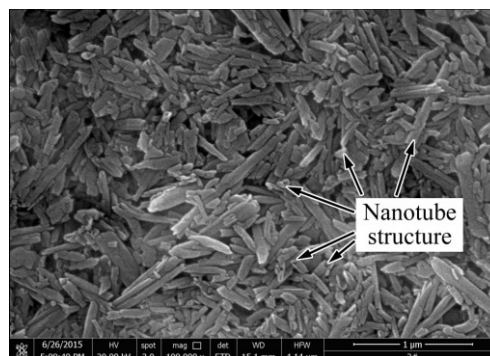


Fig. 1 SEM image of halloysite sample

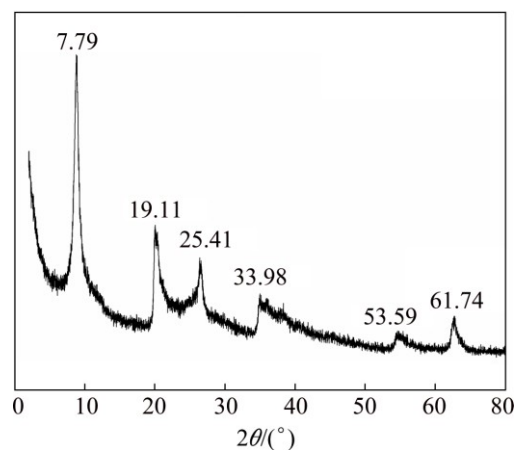


Fig. 2 X-ray diffractometer result of halloysite sample

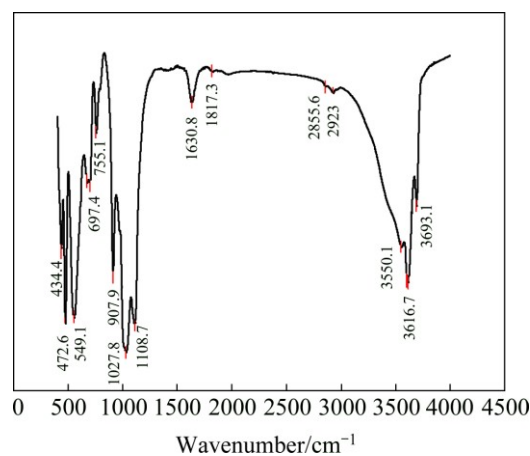


Fig. 3 FT-IR spectra of halloysite sample

Figure 1 reveals several hollow nanotube structures in the halloysite clay mineral sample, producing a high porosity, large pore volume and a high specific surface area. These properties enable ammonium to be adsorbed

on the halloysite surface. The chemical mineral composition, shown in Fig. 2, is $\text{Al}_2\text{Si}_2\text{O}_5(\text{OH})_4 \cdot 2\text{H}_2\text{O}$, which is comparable to the composition of halloysite in southern China ionic rare earth-bearing soils [1].

Figure 3 defines absorption bands at 3616.7 and 3693.1 cm^{-1} ascribed to the $-\text{OH}$ group [18,19], bands seen at 1027.8 and 1108.7 cm^{-1} and caused by the stretching vibration of $\text{Si}-\text{O}$, and a band at 907.9 cm^{-1} assigned to the bending vibration of $\text{Al}-\text{OH}$ [18]. Bands situated at 472.6 and 549.1 cm^{-1} are ascribed to $\text{Si}-\text{O}-\text{Si}$ and $\text{Al}-\text{O}-\text{Si}$ deformations, respectively, and a band located at 1630.8 cm^{-1} relates to the bending vibration of $-\text{OH}$ in water [20,21]. The FT-IR spectra result indicated several polar group minerals such as aluminum hydroxyl, silicon hydroxyl in the halloysite structure. Ion exchange and complexing could easily occur between these polar group minerals and NH_4^+-N , leading to its adsorption.

3.2 Adsorption

3.2.1 Effect of initial NH_4^+-N concentration

During in-situ leaching of the ionic rare earth ore in southern China, the content of leaching solution (ammonium sulphate) varies from high to low. At first, a high content of ammonium sulphate solution with 1%–2% is applied to leaching the rare earths, whereas a low content (close to zero) is used at the end of the leaching process. As 1% leaching solution contains 1060 mg/L of ammonium nitrogen, therefore, we considered an initial concentration range of ammonium from 0 to 1300 mg/L during this part of the experiment. The effect of the initial ammonium concentration (C_0) on the amount adsorbed by halloysite per mass unit at equilibrium (Q_e) was evaluated at $T=303$ K and $\text{pH}=5.6$, considering the in-situ leaching process and the characteristics of the mined soil. The results are presented in Fig. 4.

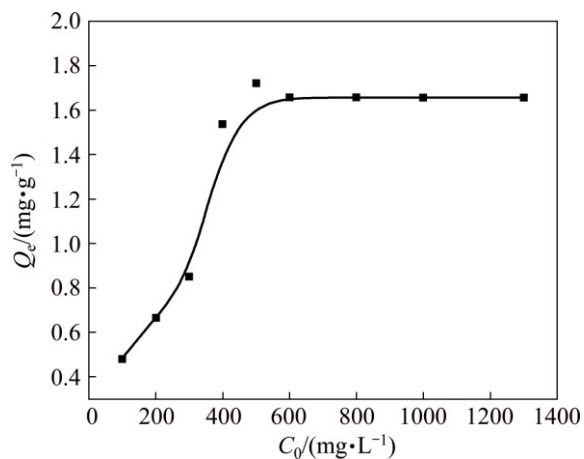


Fig. 4 Effect of initial ammonium concentration on its adsorption by halloysite clay mineral at $T=303$ K and $\text{pH}=5.6$

Figure 4 shows an increase in Q_e values with increasing C_0 when the latter is <600 mg/L. When the C_0 value reached 600 mg/L, the Q_e value attained a maximum of 1.66 mg/g; whereas for $C_0 > 600$ mg/L, the Q_e value remained stable. Figure 4 indicates that the adsorption was saturated (e.g., $Q_{e(\text{max})}$ of 1.66 mg/g) when C_0 is 600 mg/L (corresponding to a 0.57% mass ratio of ammonium sulfate, which is about half of the actual initial in-situ leaching concentration).

It could be inferred that for actual mining soil, when $T=303$ K, $\text{pH}=5.6$ and 0.57% of ammonium sulfate is applied to leach rare earths, the ammonium adsorption by mining soil can be saturated, with the saturated adsorption capacity being up to 1.66 mg/g. During the leaching process associated with mining, ammonium sulfate with 1%–2% mass ratio is commonly applied. Therefore, the adsorption of NH_4^+-N reaches saturation and some of the excess ammonium migrates in the soil water as a soluble solution.

In this segment of the experiment, the effect of contact time (t) and initial ammonium concentration (C_0) on the amount of ammonium adsorbed by the halloysite clay mineral per unit mass after contact time t , Q_t , was studied, maintaining a temperature of 303 K and a pH value of 5.6. The results are illustrated in Fig. 5.

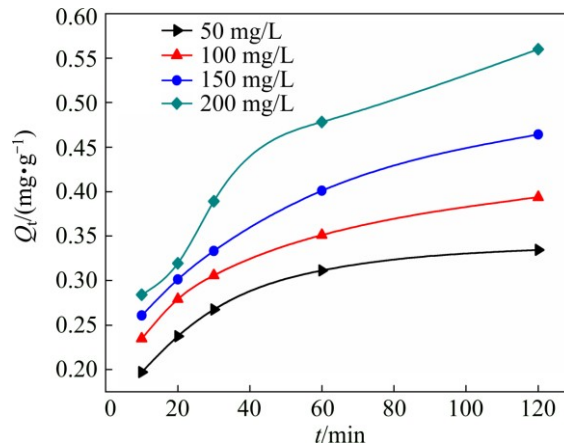


Fig. 5 Effect of contact time and initial ammonium concentration on ammonium adsorption by halloysite clay mineral at $T=303$ K, $\text{pH}=5.6$

The slope of each point from every Q_t-t curve represents the instantaneous adsorption rate (dQ_t/dt) [$\text{mg}/(\text{g}\cdot\text{s})$] (Fig. 5). The figure reveals initially a rapid increase of Q_t with time followed by a slow increase and finally approaching a platform value, resulting in a gradual diminution of the instantaneous adsorption rate (dQ_t/dt). The Q_t value at a specific time t and the instantaneous adsorption rate (dQ_t/dt) are higher under a larger initial ammonium concentration. This can be explained by an augmentation of the NH_4^+ concentration gradient between the halloysite surface and

the NH_4Cl solution as the initial NH_4^+-N concentration increases. Consequently, there is an increase of the instantaneous adsorption rate and increase of the final equilibrium adsorption capacity. Furthermore, the adsorption sites of halloysite would be surrounded by more ammonium compounds when the initial NH_4^+-N concentration increases, resulting in a rise in the adsorption rate and capacity.

3.2.2 Effect of temperature

Ionic rare earth deposit principally occurs in the first 2 to 10 m of completely weathered granitic or volcanic rocks, whereas the natural topsoil layer ammonium concentration is very low. The average annual temperature of the soil layer underneath the first 2 to 10 m of weathered rocks in southern China varies from 293 to 303 K, therefore, we studied the effect of temperature on the adsorption capacity at 288, 293, 303, and 313 K with an initial ammonium concentration (C_0) of 100 mg/L and a pH value of 5.6. The results are presented in Fig. 6.

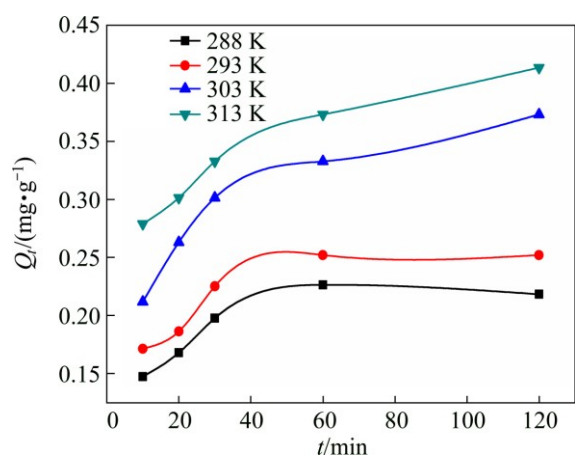


Fig. 6 Effect of contact time and temperature on ammonium adsorption by halloysite clay mineral at $C_0=100$ mg/L and $\text{pH}=5.6$

In Fig. 6, the Q_e value corresponds to the expected adsorption for each Q_t-t curve at equilibrium. Before the adsorption reached saturation, the Q_t value was larger at higher temperature, so was the Q_e value. This indicates that the ammonium adsorption by the halloysite clay mineral is favored at higher temperature. Furthermore, increasing the temperature will accelerate the flow, activity and diffusion of NH_4^+ ions in solution augmenting the likeliness of effective collisions between NH_4^+ ions and the halloysite surface and the probabilities of adsorption.

3.2.3 Effect of pH values

The effect of the pH value on the adsorption capacity is shown in Fig. 7 with a constant temperature of 303 K and an initial NH_4^+-N concentration of 100 mg/L.

The ammonium adsorption capacity grows with the pH value until it reaches about 9.0. When pH value is low, the concentration of H^+ ions in solution is high. Ion exchange and complexing would occur between H^+ ions and silicon hydroxyl or aluminum hydroxyl on the halloysite surface. Consequently, numerous adsorption sites are occupied by H^+ ions, decreasing the adsorption capacity of NH_4^+-N [22]. As the pH value augments while still lower than 9.0, the H^+ ions concentration in the solution becomes lower and the competitive adsorption of H^+ ions becomes weaker. Moreover, the surface of halloysite is more negatively charged when increasing the pH value [21]. The electrostatic attraction between positively charged NH_4^+ cations and negatively charged adsorption sites grows, generating a greater NH_4^+-N adsorption capacity. However, when the pH is > 9.0 , a hydrolysis reaction occurs described by $\text{NH}_4^+ + \text{OH}^- \rightleftharpoons \text{NH}_3 \cdot \text{H}_2\text{O}$. The hydrolysis reaction shifts to the right with a growing pH value, and the generated ammonia would be further volatilized, leading to a sharp decline in the concentration of free NH_4^+ in solution. The NH_4^+ concentration could be dramatically reduced, and the final amount of adsorption lowered substantially (Fig. 7).

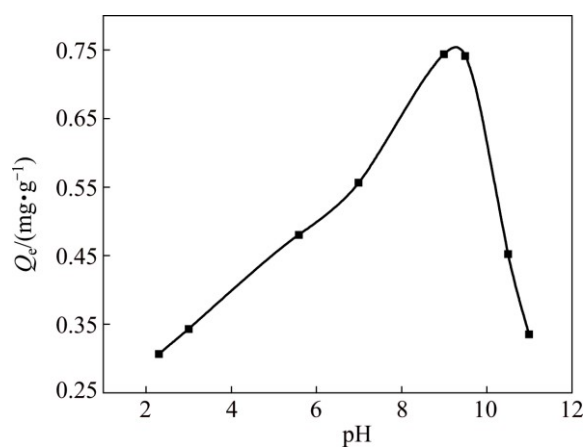


Fig. 7 Effect of pH value on ammonium adsorption by halloysite clay mineral at $T=303$ K and $C_0=100$ mg/L

The pH value in a currently mined soil is usually within a range of 4.5 to 6. Thus, its adsorption capacity for ammonium will increase with increase of the pH value.

3.3 Isothermal adsorption

Langmuir and Freundlich isothermal models [23,24] are usually adopted to analyze the liquid/solid isothermal adsorption process. The Langmuir adsorption model is based on the assumption of a monolayer adsorption on a structurally homogeneous adsorbent, where all the sorption sites are identical and energetically equivalent. When the adsorbent surface is saturated, the adsorption

capacity reaches a maximum value. The Langmuir isothermal equation is shown below [23]:

$$\frac{1}{Q_e} = \frac{1}{K_L Q_m Q_e} + \frac{1}{Q_m} \quad (3)$$

where K_L is the Langmuir constant (L/mg), Q_m is the theoretical maximum adsorption capacity corresponding to a monolayer coverage (mg/g).

The Freundlich isothermal model is an empirical equation, adequate for an adsorbent surface being non-uniform, different types of active adsorption centers, different affinities between the active centers and adsorbates and for an adsorbate ion or molecule not solely adsorbed by an active center. The Freundlich isothermal model is given by Eq. (4) [24].

$$\lg Q_e = \lg K_F + 1/n \lg C_e \quad (4)$$

where K_F is the Freundlich constant, $1/n$ is an empirical parameter related to the adsorption intensity, which varies with the heterogeneity of the material. When the value of $1/n$ lies between 0.1 and 1, the adsorption process is favored [25,26].

The Langmuir and Freundlich models are adopted to match the ammonium adsorption experiment data for the halloysite clay mineral. The results are listed in Table 1.

The correspondence between the experimental data and the model-predicted values is expressed by the correlation coefficients (R^2) (Table 1). The relatively high R^2 value is the more applicable model to the isotherm of ammonium ion adsorbed onto halloysite. In Table 1, the correlation coefficients R^2 are >0.94 , indicating the ammonium adsorption by the halloysite clay mineral is a match for both models and the adsorption is a molecular layer adsorption process on a heterogeneous surface. From the results of the Langmuir model, we observe that the theoretical maximum adsorption capacity corresponding to a monolayer coverage Q_m increases with the increase of temperature (Table 1). This confirms that elevating the temperature is favorable to the adsorption process. From the results of the Freundlich model, the $1/n$ values are less than 1, suggesting that the ammonium adsorption by halloysite occurs efficiently. We thus conclude that the ammonium adsorption process by ionic rare earth-bearing mined soils is favored and occurs as a monolayer process on a

heterogeneous surface. The adsorption capacity for ammonium would increase with an augmentation of the soil temperature.

3.4 Kinetics of adsorption

The pseudo-first-order kinetic model has been widely used to predict ion adsorption kinetics. A linear form of pseudo-first-order model is represented by Eq. (5) [27]:

$$\ln(Q_e - Q_t) = \ln Q_e - K_1 t \quad (5)$$

where K_1 is the rate constant of pseudo-first-order adsorption (min^{-1}).

The pseudo-second-order kinetic model is also commonly applied to the description of the kinetics of ion adsorption. The linear form is represented by Eq. (6) [28]:

$$\frac{1}{Q_t} = \frac{1}{K_2 Q_e^2} + \frac{t}{Q_e} \quad (6)$$

where K_2 is the rate constant of the pseudo-second-order adsorption ($\text{g}/(\text{mg} \cdot \text{min})$).

The intra-particle diffusion model [29] is another one commonly used for the ion adsorption process, thus,

$$Q_t = K_p t^{1/2} \quad (7)$$

where, K_p is the intra-particle diffusion rate constant ($\text{mg}/(\text{g} \cdot \text{min}^{0.5})$).

The three kinetic models are applied to matching the experiment data, and the results are presented in Fig. 8.

The pseudo-first-order model correlation coefficients (R^2) values are 0.464, 0.565, 0.955 and 0.980 at 288, 293, 303 and 313 K, respectively (Fig. 8(a)), suggesting that the ammonium adsorption by halloysite can be matched by the pseudo-first-order kinetic model except at lower temperature. Film diffusion is the important controlling factor of the pseudo-first-order model, therefore, the ammonium adsorption by halloysite could be affected by the resistance to film diffusion. However, the latter was not the only influencing factor because the intercepts of the fitting lines were not equal to zero (Fig. 8(a)) [30]. The R^2 values in Fig. 8(c) lines are 0.645, 0.672, 0.967 and 0.918, respectively,

Table 1 Langmuir and Freundlich isotherm parameters for ammonium adsorption by halloysite

T/K	Langmuir				Freundlich			
	Fitting equation	$K_L/(\text{L} \cdot \text{mg}^{-1})$	$Q_m/(\text{mg} \cdot \text{g}^{-1})$	R^2	Fitting equation	$K_F/(\text{L} \cdot \text{mg}^{-1})$	$1/n$	R^2
288	$b=45.838a+1.946$	0.0425	0.514	0.944	$y=0.423x-1.242$	0.0573	0.423	0.981
293	$b=45.723a+1.815$	0.0397	0.551	0.947	$y=0.442x-1.254$	0.0557	0.442	0.987
303	$b=44.635a+1.507$	0.0337	0.664	0.956	$y=0.494x-1.285$	0.0519	0.494	0.998
313	$b=43.885a+1.356$	0.0309	0.737	0.966	$y=0.513x-1.286$	0.0518	0.513	0.993

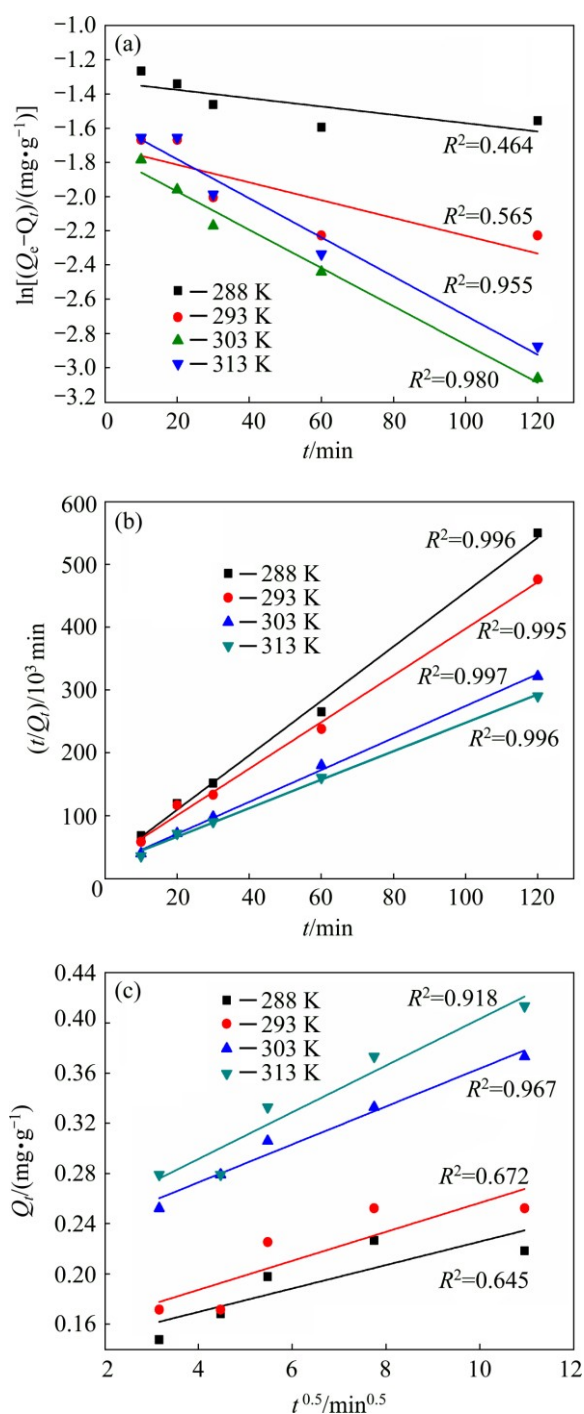


Fig. 8 Kinetics of ammonium adsorption by halloysite clay mineral at different temperatures, with $C_0 = 100$ mg/L and pH=5.6: (a) Pseudo-first-order model plot; (b) Pseudo-second-order model plot; (c) Intra-particle diffusion model plot

suggesting the ammonium adsorption by halloysite generally agrees with the intra-particle diffusion model, except at lower temperature. However, the fitting lines did not intersect the Y-axis at zero point, thus indicating that intra-particle diffusion is not the only controlling factor [31].

The correlation coefficients values shown in

Fig. 8(b) are 0.996, 0.995, 0.997 and 0.996 at different temperatures, respectively. This demonstrates that the ammonium adsorption process by the halloysite clay mineral corresponds to a pseudo-second-order kinetic equation. The formation of chemical bonds remains the principal controlling factor for the pseudo-second-order adsorption model, therefore, we can infer that the ammonium adsorption by halloysite mainly belongs to a chemical adsorption. Furthermore, surface adsorption and intra-particle diffusion are also involved in the pseudo-second-order model [32], the adsorption was kinetically controlled by external film diffusion, surface adsorption and intra-particle diffusion.

4 Conclusions

1) At a temperature of 303 K and a pH value of 5.6, when the initial concentration of ammonium reached 600 mg/L, the ammonium adsorption by the halloysite clay mineral showed saturation. Therefore, when the concentration of the ammonium sulfate leaching solution reached 0.57% during in-situ leaching practice of ionic rare earth ore, the maximum ammonium adsorption capacity of the mined soil could be obtained with a value of about 1.66 mg/g.

2) When the initial concentrations of $NH_4^+ - N$, the pH values (3.0 to 6.0) and the temperatures (288 K to 313 K) increased, the ammonium adsorption capacity by the halloysite clay mineral and by the mined soil increased, before the adsorption reached saturation.

3) The isothermal ammonium adsorption by halloysite matched the Langmuir and Freundlich isotherms. The ammonium adsorption of ionic rare earth-bearing mined soils favored a monolayer process on a heterogeneous surface.

4) The ammonium adsorption process of ionic rare earth-bearing mined soils was believed to follow a pseudo-second kinetic equation and was kinetically controlled by liquid film diffusion, surface adsorption and intra-particle diffusion.

References

- [1] CHI R A, TIAN J, LI Z J, PENG C, WU Y X, LI S R, WANG C W, ZHOU Z H. Existing state and partitioning of rare earth on weathered ores [J]. *Journal of Rare Earths*, 2005, 23(6): 756–759.
- [2] QIU T S, FANG X H, WU H Q, ZENG Q H, ZHU D M. Leaching behaviors of iron and aluminum elements of ion-absorbed-rare-earth ore with a new impurity depressant [J]. *Transactions of Nonferrous Metals Society of China*, 2014, 24: 2986–2990.
- [3] TIAN J, TANG X K, YIN J Q, CHEN J, LUO X P, RAO G H. Enhanced leachability of a lean weathered crust elution-deposited rare-earth ore: Effects of sesbania gum filter-aid reagent [J]. *Metallurgical and Materials Transactions B*, 2013, 44(5): 1070–1077.
- [4] HUANG X W, LONG Z Q, WANG L S, FENG Z Y. Technology

- development for rare earth cleaner hydrometallurgy in China [J]. *Rare Metals*, 2015, 34(4): 215–222.
- [5] XIAO Y, FENG Z, HU G, HUANG L, HUANG X, CHEN Y, LI M. Leaching and mass transfer characteristics of elements from ion-adsorption type rare earth ore [J]. *Rare Metals*, 2015, 34(5): 357–365.
- [6] TANG C J, ZHENG P, CHAI L Y, MIN X B. Characterization and quantification of anammox start-up in UASB reactors seeded with conventional activated sludge [J]. *International Biodeterioration & Biodegradation*, 2013, 82: 141–148.
- [7] ALI M, CHAI L Y, MIN X B, TANG C J, AFRIN S, LIAO Q, WANG H Y, PENG C, SONG Y X, ZHENG P. Performance and characteristics of a nitrification air-lift reactor under long-term HRT shortening [J]. *International Biodeterioration & Biodegradation*, 2016, 111: 45–53.
- [8] PENG C, CHAI L Y, TANG C J, MIN X B, SONG Y X, DUAN C S, YU C. Study on the mechanism of copper-ammonia complex decomposition in struvite formation process and enhanced ammonia and copper removal [J]. *Journal of Environmental Sciences*, 2017, 51(1): 222–233.
- [9] Jiangxi Province Water Resources Department, Jiangxi Province Bureau of Hydrology, Municipal Water Resources (Water) Bureau, City (Poyang Lake) Hydrological Bureau. *Jiangxi Water Resources Bulletin* [R]. 2014. (in Chinese)
- [10] Jiangxi Province Water Resources Department, Jiangxi Province Bureau of Hydrology, Municipal Water Resources (Water) Bureau, City (Poyang Lake) Hydrological Bureau. *Jiangxi Water Resources Bulletin* [R]. 2013. (in Chinese)
- [11] YU J G, ZHAO X H, YANG H, CHEN X H, YANG Q, YU L Y, JIANG J H, CHEN X Q. Aqueous adsorption and removal of organic contaminants by carbon nanotubes [J]. *Science of the Total Environment*, 2014, 482–483(1): 241–251.
- [12] WANG T, ZHANG L Y, LI C F, YANG W C, SONG T T, TANG C J, MENG Y, DAI S, WANG H Y, CHAI L Y, LUO J. Synthesis of core-shell magnetic Fe_3O_4 @poly (m-Phenylenediamine) particles for chromium reduction and adsorption [J]. *Environ Sci Technol*, 2015, 49 (9): 5654–5662.
- [13] WANG J H, ZHANG X, ZHANG B, ZHAO Y, ZHAI R, LIU J, CHEN R. Rapid adsorption of Cr (VI) on modified halloysite nanotubes [J]. *Desalination*, 2010, 259: 22–28.
- [14] KIANI G. High removal capacity of silver ions from aqueous solution onto halloysite nanotubes [J]. *Applied Clay Science*, 2014, 90: 159–164.
- [15] LI J, WEN F, PAN L, LIU Z, DONG Y. Removal of radiocobalt ions from aqueous solutions by natural halloysite nanotubes [J]. *Journal of Radioanalytical and Nuclear Chemistry*, 2013, 295: 431–438.
- [16] VISERAS M T, AGUZZI C, CEREZO P, VISERAS C, VALENZUELA C. Equilibrium and kinetics of 5-aminosalicylic acid adsorption by halloysite [J]. *Microporous and Mesoporous Materials*, 2008, 108: 112–116.
- [17] KIANI G, DOSTALI M, ROSTAMI A, KHATAEE A R. Adsorption studies on the removal of Malachite Green from aqueous solutions onto halloysite nanotubes [J]. *Applied Clay Science*, 2011, 54: 34–39.
- [18] WANG J, ZHANG X, ZHANG B, ZHAO Y, ZHAI R, LIU J, CHEN R. Rapid adsorption of Cr (VI) on modified halloysite nanotubes [J]. *Desalination*, 2010, 259: 22–28.
- [19] BARRIENTOS R S, de OCA R G M, RAMOS F E V, SEPULVEDA E A, PASTOR B M M, GONZALEZ M A. Surface modification of natural halloysite clay nanotubes with aminosilanes: Application as catalyst supports in the atom transfer radical polymerization of methyl methacrylate [J]. *Applied Catalysis A: General*, 2011, 406: 22–33.
- [20] PENG Y, PETER S D, LIU Z, MALCOLM E R G, HOOK J M, ANTILL S A, KEPERT C J. Functionalization of halloysite clay nanotubes by grafting with γ -aminopropyltriethoxysilane [J]. *The Journal of Physical Chemistry C*, 2008, 112(40): 15742–15751.
- [21] HU C, CHEN Y, ZHANG W, WANG P, WANG J. Adsorption performance of Co(II) on magnetic halloysite [J]. *Acta Scientiae Circumstantiae*, 2015, 35(9): 2813–2819. (in Chinese)
- [22] EL-SHAFFEY O I, FATHY N A, EL-NABARAWY T A. Sorption of ammonium ions onto natural and modified Egyptian kaolinites: Kinetic and equilibrium studies [J]. *Advances in Physical Chemistry*, 2014: 1–12.
- [23] XIA L, HU Y, ZHANG B. Kinetics and equilibrium adsorption of copper(II) and nickel(II) ions from aqueous solution using sawdust xanthate modified with ethanediamine [J]. *Transactions of Nonferrous Metals Society of China*, 2014, 24: 868–875.
- [24] WU Z, HUA Z, YUAN X, WANG H(1), WANG L, CHEN X, ZENG G, WU Y. Adsorptive removal of methylene blue by rhamnolipid-functionalized graphene oxide from wastewater [J]. *Water Research*, 2014, 67: 330–344.
- [25] YANG J, ZENG Q R, PENG L, LEI M, SONG H J, TIE B Q, GU J D. La-EDTA coated Fe_3O_4 nanomaterial: Preparation and application in removal of phosphate from water [J]. *Journal of Environmental Sciences*, 2013, 25(2): 413–418.
- [26] DAI J, REN F L, TAO C Y. Adsorption of Cr(VI) and speciation of Cr(VI) and Cr(III) in aqueous solutions using chemically modified chitosan [J]. *International Journal of Environmental Research & Public Health*, 2012, 9(5): 1757–1770.
- [27] LAGERGREN S. About the theory of so-called adsorption of soluble substances [J]. *The Royal Swedish Academy of Sciences Documents*, 1898, 24(4): 1–39.
- [28] YU W, CHAI L, ZHANG L, WANG H. Synthesis of poly (m-phenylenediamine) with improved properties and superior prospect for Cr(VI) removal [J]. *Transactions of Nonferrous Metals Society of China*, 2013, 23: 3490–3498.
- [29] WEBER W J, MORRIS J C. Kinetics of adsorption on carbon from solution [J]. *Journal of the Sanitary Engineering Division, American Society of Civil Engineers*, 1963, 89(17): 31–60.
- [30] BO J, WANG Q, QIN H, ZHENG G, YANG Y, GUAN X. Kinetics and thermodynamics of adsorption of heavy metal ions onto fly ash from oil shale [J]. *Journal of Fuel Chemistry and Technology*, 2011, 39(5): 378–386. (in Chinese)
- [31] ZHANG Q L, GAO N Y, LIN Y C, XU B, LE L S. Removal of arsenic(V) from aqueous solutions using iron-oxide-coated modified activated carbon [J]. *Water Environment Research*, 2007, 79(8): 931–936.
- [32] CHANG M Y, JUANG R S. Adsorption of tannic acid, humic acid, and dyes from water using the composite of chitosan and activated clay [J]. *Journal of Colloid and Interface Science*, 2004, 278(1): 18–25.

埃洛石粘土矿物对氨氮的吸附规律

靖青秀^{1,2}, 柴立元¹, 黄晓东², 唐崇俭¹, 郭欢², 王巍²

1. 中南大学 冶金与环境学院, 长沙 410083;

2. 江西理工大学 冶金与化学工程学院, 赣州 341000

摘要: 中国南方离子型稀土矿区土壤氨氮污染日趋严重。埃洛石是矿区土壤的主要粘土成分之一。研究了埃洛石对氨氮的饱和吸附量、吸附影响因素及其吸附动力学特点。结果表明: 在 $T=303\text{ K}$ 、 $\text{pH}=5.6$ 条件下, 氨氮初始浓度增至 600 mg/L 左右(接近原地浸矿工艺实际使用的最初浸矿剂浓度的 $1/2$)时, 埃洛石和矿区土壤对氨氮的吸附达饱和, 饱和吸附量为 1.66 mg/g 左右; 随 NH_4^+-N 初始浓度、 pH 值($3.0\sim 6.0$)、温度($288\sim 313\text{ K}$)的升高, 埃洛石及矿区土壤对氨氮的吸附量增大; 埃洛石对氨氮的吸附符合 Langmuir 等温方程和 Freundlich 等温方程, 可近似认为离子型稀土矿区土壤对氨氮的吸附易于进行; 埃洛石对氨氮的吸附过程符合准二级动力学方程。

关键词: 离子型稀土矿区; 埃洛石; 氨氮污染; 吸附; 动力学

(Edited by Yun-bin HE)